Journal of the Iranian Chemical Society
https://doi.org/10.1007/s13738-020-02069-9

ORIGINAL PAPER

Magnetite (Fe_3O_4) nanoparticles-supported dodecylbenzenesulfonic acid as a highly efficient and green heterogeneous catalyst for the synthesis of substituted quinolines and 1-amidoalkyl-2-naphthol derivatives

Deepak Katheriya[1] · Nipun Patel[1] · Harsh Dadhania[2] · Abhishek Dadhania[1]

Received: 14 June 2020 / Accepted: 18 September 2020

Abstract

Magnetically retrievable, magnetite (Fe_3O_4) nanoparticles-supported dodecylbenzenesulfonic acid (DDBSA@MNP) was synthesized and characterized through different analytical techniques such as TEM, XRD, FTIR, TGA, SEM, EDX and VSM. The catalytic efficiency of synthesized DDBSA@MNP was evaluated for the synthesis of substituted quinolines and 1-amidoalkyl-2-naphthols through one-pot condensation. The methodology provides a facile approach for the synthesis of targeted compounds with excellent isolated yields. Additionally, the catalyst can be recovered through external magnet and reused up to five reaction cycles with prominent reactivity. The present approach offers many advantages such as green and mild reaction condition, facile catalyst recovery and excellent isolated yield of final products.

Graphic abstract

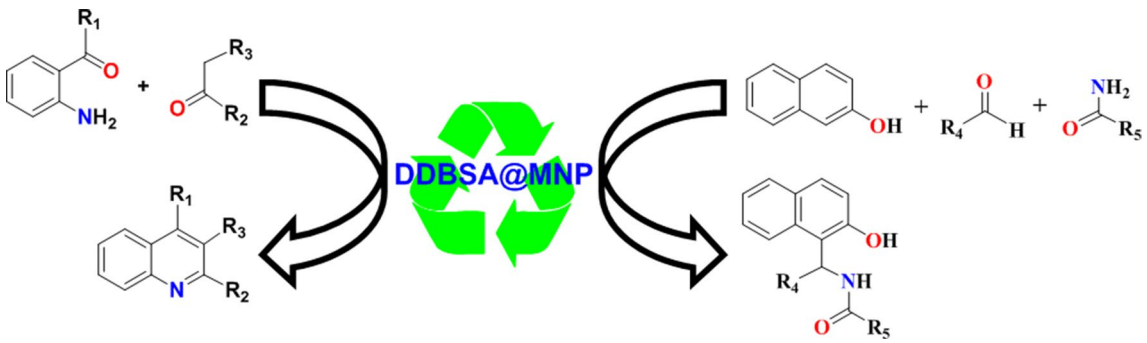

Keywords Magnetic nanoparticles · Heterogeneous catalyst · One-pot condensation · Friedlander reaction

Introduction

Homogeneous catalysts have been known for several years due to their distinct features such as high activity and selectivity [1–3]. Homogeneous nature of the catalyst renders all catalytic sites available for the reactants and also provides the stereo- and regioselectivity to the reaction [4]. However, homogeneous catalysts contribute not more than 15% of the industrial processes as compared to its counterpart heterogeneous catalysts [5]. The reason behind this trend is difficulties associated with their separation and reusability.

Electronic supplementary material The online version of this article (https://doi.org/10.1007/s13738-020-02069-9) contains supplementary material, which is available to authorized users.

✉ Abhishek Dadhania
abhishekdadhania.bt@charusat.ac.in

[1] Department of Chemical Sciences, P. D. Patel Institute of Applied Sciences, Charotar University of Science and Technology (CHARUSAT), Changa, Gujarat 388421, India

[2] Department of Chemistry, Sardar Patel University, Vallabh Vidyanagar 388120, Gujarat, India

Published online: 28 September 2020

Separation of trace amount of catalysts from final product is very much important, especially in highly regulated pharmaceutical sector [6]. Likewise, reusability is directly related to sustainability of the process and has a huge impact on product cost and pollution. Even after utilization of different experimental techniques such as extraction, distillation and chromatography, the catalyst separation remains a huge challenge [7]. An ideal solution for this problem is heterogenization of homogeneous catalyst through its immobilization on solid supports such as polymer, silica, carbon and some metal oxides [8–12]. However, heterogenization usually lowers its catalytic efficiency as it limits the access of catalytic sites for reactants. In order to overcome this drawback, porous material such as zeolite has been utilized as a solid support [13, 14]. Another way to tackle this issue is to use nano-size solid support for the immobilization of catalyst. The higher surface area of nanomaterial will enhance the accessibility of catalytic sites for reactants [15]. However, due to nanometer size the separation of catalyst through filtration is cumbersome. The feasible solution for this issue is to utilize magnetic nanoparticles (MNPs) as a solid support for immobilization of homogeneous catalyst. MNPs emerged as an ideal support due to their distinct features such as easy synthesis, lower toxicity and cost, higher stability and most importantly its paramagnetic nature, which provides an easy separation through external magnet [16–19].

The Friedlander reaction is the condensation of 2-aminoaryl ketones and β-ketoester followed by a cyclodehydration reaction [20]. Quinoline is the product of this condensation, which has great impact on pharmaceutical and agrochemical industries due to its attractive biological activities [21]. Furthermore, quinoline is an important moiety widely present in many natural products [22, 23]. The structural nuclei based on quinoline can serve in compounds with comprehensive biological activities including anti-tumor [24, 25], anticancer [26, 27], antiplasmodial [23], analgesic [28], anti-bacterial [29, 30], fungicidal [31], anti-allergic [32], antimalarial [33], antimicrobial [34], anti-inflammatory [35] and anti-tubercular [36]. Many reports were published on the Friedlander reaction using different homogeneous as well as heterogeneous catalysts [37–42]. Likewise, 1-amidoalkyl-2-naphthols have emerged as privileged medicinal scaffolds due to their hydrolyzed product 1-aminoalkyl-2-naphthols, which possess attractive biological activities such as bradycardic and hypotensive effects [43]. Moreover, these 1,3-amino-oxygenated derivatives are ubiquitous and found in many natural products and drug molecules such as ritonavir and lopinavir [44–46]. Owing to important medicinal properties, many synthetic methods are reported for the synthesis of 1-amidoalkyl-2-naphthols via a one-pot multicomponent reaction between 2-naphthol, aldehydes and amides using different catalysts [47–52]. However, the use of excessive catalyst, strong acidic condition, use of toxic and expensive metal catalyst, longer reaction time, lower to moderate yields and poor recovery and reusability of catalyst limits the scope for some of these methodologies for the synthesis of quinolines and 1-amidoalkyl-2-naphthol derivatives. Hence, a facile and efficient strategy using sustainable catalyst is required for the synthesis of these derivatives.

In this contribution, we report the utilization of magnetite nanoparticles-supported dodecylbenzenesulfonic acid (DDBSA@MNP) as a catalyst for the synthesis of substituted quinolines (Scheme 1) and 1-amidoalkyl-2-naphthol derivatives (Scheme 2). The catalyst was found highly efficient, eco-friendly, magnetically separable and reusable to obtained corresponding products in excellent yields.

Scheme 1 DDBSA@MNP-catalyzed synthesis of substituted quinolines

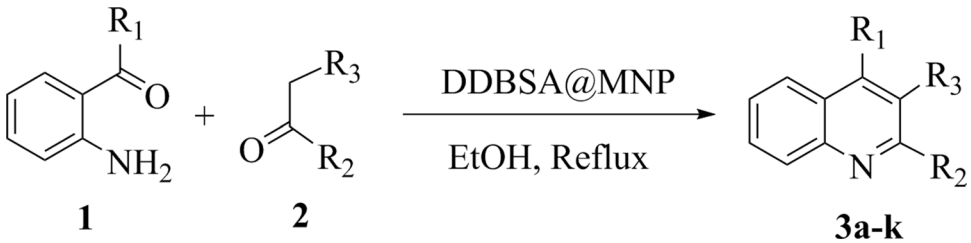

Scheme 2 DDBSA@MNP-catalyzed synthesis of 1-amidoalkyl-2-naphthols

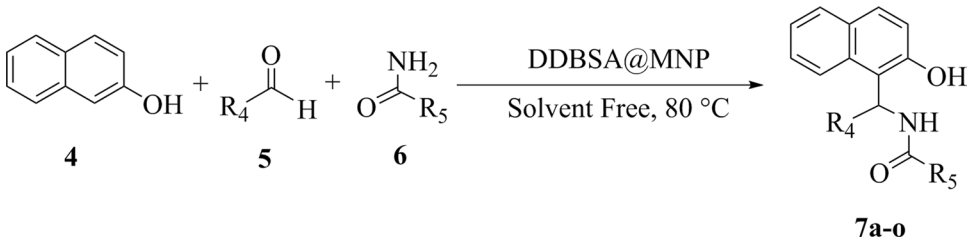

Experimental

Materials and instruments

All the chemicals and reagents were purchased from the commercial sources and used without further purification. Melting points were determined through VMP-D melting point apparatus and were uncorrected. A Thermo Nicolet 6700 spectrophotometer was used to record FTIR spectra using KBr pellets. TG analysis was performed on a Mettler Toledo thermal analyzer under nitrogen atmosphere. A Bruker D2 phaser bench-top diffractometer was used to record X-ray diffraction pattern. TEM images were recorded on a JEOL JEM 2100 instrument. FESEM micrographs were recorded using a JEOL JSM-7100F instrument. VSM-7400, Lake Shore, USA, was used to record magnetization curves. ^{1}H and ^{13}C NMR spectra were recorded on a 400 MHz Bruker Avance spectrometer. EDX spectrum was recorded on a JEOL JSM-5610 scanning electron microscope.

Synthesis of silica-coated Fe_3O_4 nanoparticles ($SiO_2@Fe_3O_4$)

Magnetite (Fe_3O_4) nanoparticles were synthesized through co-precipitation method [53]. Initially, $FeCl_3{\cdot}6H_2O$ (5.4 g) and NH_2CONH_2 (3.6 g) were dissolved in water (200 mL) and kept at 90 °C for 2 h to turn the solution brown. After that, $FeSO_4{\cdot}7H_2O$ (2.8 g) was added to the mixture at room temperature and 0.1 M NaOH solution was added drop wise to adjust the pH of resultant solution at 10. The precipitates were sonicated for 30 min and kept aside for 5 h at room temperature. The obtained black powder was washed with water and dried under vacuum. The obtained Fe_3O_4 nanoparticles were dispersed in the mixture of ethanol and water (80:20) through sonication for 1 h. After that, concentrated $NH_3{\cdot}H_2O$ (5 mL) and TEOS (5 mL) were added to the dispersion and stirred vigorously for 24 h to obtain silica-coated Fe_3O_4 nanoparticles and washed with ethanol and dried under vacuum.

Synthesis of DDBSA@MNP catalyst

Silica-coated Fe_3O_4 nanoparticles were decorated with dodecylbenzenesulfonic acid to attain the DDBSA@MNP. Initially, $SiO_2@Fe_3O_4$ nanoparticles (1 g) were added in MeOH (25 mL) and sonicated for 60 min to get proper dispersion. DDBSA (1.04 mL) was added to the dispersion, and the solution was refluxed for 4 h. Solvent was removed through reduced pressure, and resulting powder was dried at 110 °C for 2 h to get DDBSA@MNP.

General procedure for the synthesis of substituted quinoline derivatives

A mixture of the 2-aminoaryl ketone (1 mmol), β-ketoester/ketone (1.5 mmol) and DDBSA@MNP (0.15 g) in EtOH (5 mL) was stirred under reflux condition for appropriate time as indicated by TLC. After completion of the reaction, the catalyst was separated through magnetic decantation, thoroughly washed with ethanol and dried under vacuum for its further use in next reaction cycle. The crude product was purified over silica gel to obtain pure quinoline derivatives. Afforded products were characterized by their melting points, ^{1}H and ^{13}C NMR data and found in agreement with the literature. The spectral data of representative quinoline derivatives are given in the following.

Ethyl 2-methyl-4-phenylquinoline-3-carboxylate (3a) ^{1}H NMR (400 MHz, $CDCl_3$) δ (ppm): 0.98 (t, 3H), 2.80 (s, 3H), 4.07(q, 2H), 7.37–7.39 (m, 2H), 7.42–7.49 (m, 4H), 7.59 (d, 1H), 7.73 (t, 1H), 8.09 (d, 1H); ^{13}C NMR δ: 8.88, 19.05, 56.57, 120.43, 121.66, 121.75, 122.68, 123.47, 123.69, 123.85, 124.12, 124.65, 125.49, 131.02, 141.52, 142.98, 149.88, 163.70.

Methyl 2-methyl-4-phenylquinoline-3-carboxylate (3b) ^{1}H NMR (400 MHz, $CDCl_3$) δ (ppm): 2.79 (s, 3H), 3.59 (s, 3H), 7.29 (s, 2H), 7.37–7.51 (m, 4H), 7.60 (d, 1H), 7.74 (t, 1H), 8.10 (d, 1H); 13C NMR δ: 23.81, 52.14, 125.09, 126.46, 126.53, 127.28, 128.27, 128.49, 128.89, 129.25, 129.40, 130.31, 135.69, 146.40, 147.78, 154.55, 169.00.

1-(2-Methyl-4-phenylquinolin-3-yl)ethanone (3c) ^{1}H NMR (400 MHz, $CDCl_3$) δ (ppm): 2.02 (s, 3H), 2.72 (s, 3H), 7.37 (s, 2H), 7.38 (d, 1H), 7.46–7.54 (m, 3H), 7.64 (d, 1H), 7.76 (t, 1H), 8.10 (d, 1H); ^{13}C NMR δ: 24.10, 31.84, 121.70, 124.08, 126.17, 126.53, 128.72, 128.89, 128.91, 130.06, 130.11, 135.23, 145.33, 155.96, 195.42.

9-Phenyl-1,2,3,4-tetrahydroacridine (3e) ^{1}H NMR (400 MHz, $CDCl_3$) δ (ppm): 1.78–1.86 (m, 2H), 1.92–2.02 (m, 2H), 2.62 (t, 2H), 3.22 (t, 2H), 7.26 (t, 2H), 7.32 (d, 2H), 7.46–7.64 (m, 4H), 8.04 (d, 1H); ^{13}C NMR δ: 22.02, 23.21, 28.57, 34.81, 120.81, 122.89, 125.36, 125.79, 126.68, 127.72, 128.34, 128.40, 128.61, 129.12, 137.23, 144.99, 146.70, 159.20.

3,3,9-Trimethyl-3,4-dihydroacridin-1(2H)-one (3k) ^{1}H NMR (400 MHz, $CDCl_3$) δ (ppm): 1.14 (s, 6H), 2.67 (s, 2H), 3.07 (s, 3H), 3.18 (s, 2H), 7.57 (t, 1H), 7.77 (t, 1H), 8.00 (d, 1H), 8.22 (d, 1H); ^{13}C NMR δ: 15.98, 28.31, 32.12, 48.59, 54.86, 124.17, 125.54, 126.37, 127.64, 129.21, 131.45, 148.29, 149.69, 161.09, 200.69.

General procedure for the synthesis of 1-amidoalkyl-2-naphthol derivatives

In a typical procedure, a round-bottom flask was charged with 2-naphthol (1 mmol), aldehyde (1 mmol), amide (1.2 mmol) and DDBSA@MNP (0.15 g). The reaction mixture was stirred at 80 °C till the completion of reaction as monitored by TLC. After the completion of reaction, hot water was added to the reaction mixture to remove unreacted water-soluble starting materials. After that, solid residue was dissolved in EtOH and catalyst was easily separated through external magnet, washed with ethanol and dried under vacuum to reuse in the next cycle. The solution was concentrated to get crude residue and was purified by recrystallization to afford final product. All the synthesized compounds were characterized through their melting points, ^{1}H and ^{13}C NMR data and matched well with the reported data. The spectral data for some selected compounds are given in the following.

N-((2-Hydroxynaphthalen-1-yl)(phenyl)methyl)acetamide (7a) ^{1}H NMR (400 MHz, DMSO) δ (ppm): 1.98 (s, 3H), 7.12–7.36 (m, 9H), 7.76–7.82 (m, 3H), 8.45 (d, 1H), 10.00 (s, 1H); ^{13}C NMR δ: 23.13, 48.28, 118.94, 119.32, 122.84, 123.77, 126.32, 126.75, 128.43, 128.92, 129.00, 129.68, 132.79, 143.09, 153.61, 169.67.

N-((2-Hydroxynaphthalen-1-yl)(phenyl)methyl)-benzamide (7j) ^{1}H NMR (400 MHz, DMSO) δ (ppm): 7.20–7.30 (m, 8H), 7.49–7.55 (m, 4H), 7.79–7.88 (m, 4H), 8.10 (d, 1H), 9.02 (s, 1H), 10.34 (s, 1H); ^{13}C NMR δ: 49.71, 109.11, 118.83, 119.17, 123.15, 126.56, 126.92, 127.01, 127.23, 127.61, 127.92, 128.66, 128.86, 128.98, 129.09, 129.75, 129.84, 131.90, 132.79, 134.82, 142.49, 153.66, 166.22.

N-((4-Chlorophenyl)(2-hydroxynaphthalen-1-yl)methyl) benzamide (7k) ^{1}H NMR (400 MHz, DMSO) δ (ppm): 7.25–7.36 (m, 7H), 7.46–7.57 (m, 4H), 7.80–7.89 (m, 4H), 8.08 (d, 1H), 9.04 (d, 1H), 10.38 (s, 1H); ^{13}C NMR δ: 49.25, 118.38, 119.15, 123.19, 127.32, 127.50, 128.01, 128.59, 128.82, 129.13, 130.15, 131.94, 132.72, 134.68, 141.58, 153.78, 166.37.

N-((2-Hydroxynaphthalen-1-yl)(2-nitrophenyl)methyl)-benzamide (7l) ^{1}H NMR (400 MHz, DMSO) δ (ppm): 7.13 (d,1H), 7.29 (t, 1H), 7.42–7.52 (m, 6H), 7.62 (t, 1H), 7.74–7.90 (m, 6H), 7.99 (d, 1H), 9.09 (d, 1H), 9.90 (s, 1H); ^{13}C NMR δ: 47.20, 116.20, 119.10, 122.95, 124.63, 127.08, 128.11, 128.40, 128.71, 128.99, 129.81, 130.34, 131.82, 132.70, 133.56, 136.32, 149.53, 154.45, 166.43.

N-((2-Hydroxynaphthalen-1-yl)(3-nitrophenyl)methyl)-benzamide (7m) ^{1}H NMR (400 MHz, DMSO) δ (ppm): 7.27 (d, 2H), 7.33 (t, 1H), 7.41 (d, 3H), 7.49 (t, 2H), 7.73 (d, 1H), 7.84–7.92 (m, 4H), 8.11 (t, 3H) 9.16 (d, 1H), 10.40 (s, 1H); ^{13}C NMR δ: 49.43, 117.78, 119.10, 121.44, 122.11, 123.01, 127.51, 128.87, 129.22, 130.23, 130.47, 132.04, 132.69, 133.78, 134.50, 145.03, 148.28, 153.93, 166.72.

Results and discussion

Synthesis and characterization of DDBSA@MNP

Magnetite (Fe_3O_4) nanoparticles-supported catalyst was prepared in a three-step procedure as shown in Scheme 3.

Initially, Fe_3O_4 nanoparticles were synthesized by a co-precipitation method, and then, it underwent surface coating with tetraethyl orthosilicate (TEOS) under alkaline condition to acquire silica-coated magnetite nanoparticles (SiO_2@Fe_3O_4) in an almost quantitative yield. Synthesized SiO_2@Fe_3O_4 nanoparticles were used as solid support for the grafting of dodecylbenzenesulfonic acid (DDBSA). The successful grafting was confirmed through the appearance of the characteristic band around 1450 cm^{-1} for S=O stretching and strong band around 2925 cm^{-1} for C–H stretching in FTIR spectrum and also supported by the presence of S in EDX spectrum. The loading of DDBSA was determined through TG analysis and was found to be 0.56 mmol g^{-1}.

The crystalline nature of the Fe_3O_4 nanoparticles was identified with XRD (Fig. 1). The peak positions and relative intensities match well with XRD pattern of magnetite nanoparticles in the literature (JCPDS card no. 01-1111) [54]. The same characteristic peaks were observed in the XRD pattern of SiO_2@Fe_3O_4 and DDBSA@MNP,

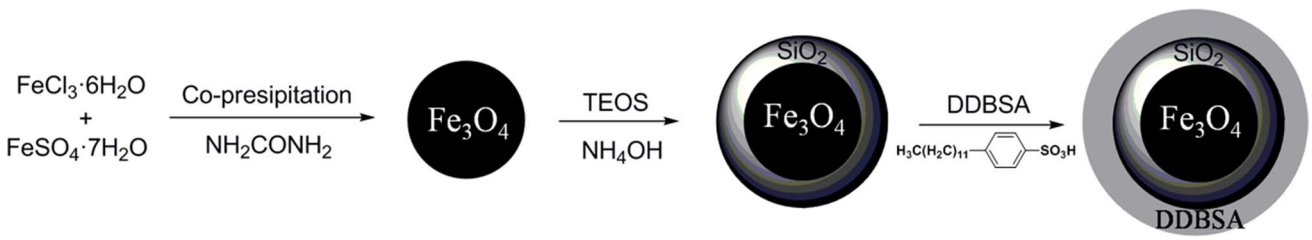

Scheme 3 Synthesis of DDBSA@MNP

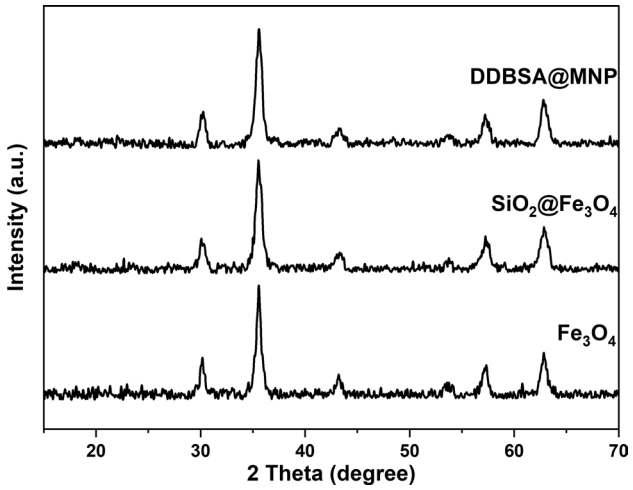

Fig. 1 XRD patterns of Fe_3O_4, SiO_2@Fe_3O_4 and DDBSA@MNP

showing the crystallinity of both materials after functionalization (Fig. 1). The particle size of the DDBSA@MNP calculated using the Scherrer equation is 15.37 nm, which is in accordance with the particle size obtained from the TEM analysis.

Transmission electron microscopy (TEM) was used to check morphology of the catalyst. TEM images show the core–shell structure of the catalyst with an average particle size of ~ 16 nm (Fig. 2). The selected-area electron diffraction (SAED) pattern confirms the polycrystalline nature of the nanoparticles. The core–shell morphology of the dodecylbenzenesulfonic acid-coated magnetite nanoparticles was corroborated by TEM images of DDBSA@MNP.

FTIR spectroscopy was used to confirm the silica coating and grafting of DDBSA on magnetite nanoparticles. FTIR spectra of SiO_2@Fe_3O_4 and DDBSA@MNP are shown in Fig. 3. Both the spectra show broad bands around 3410 and 1630 cm^{-1} due to hydroxyl group of adsorbed water [55]. Characteristic band of Fe–O bond observed around 580 cm^{-1} in both spectra confirms the presence of magnetite core [56]. Silica coating on magnetite core shows a characteristic band due to stretching and bending vibrations of Si–O–Si around 1100 cm^{-1}, along with shoulder around 1200 and 460 cm^{-1} [57]. The grafting of DDBSA was confirmed through characteristic band for S=O around 1172 cm^{-1} and band for C–H stretching vibrations around 2855 and 2925 cm^{-1} [58].

Surface morphology of the DDBSA@MNP was characterized by the field emission scanning electron microscopy

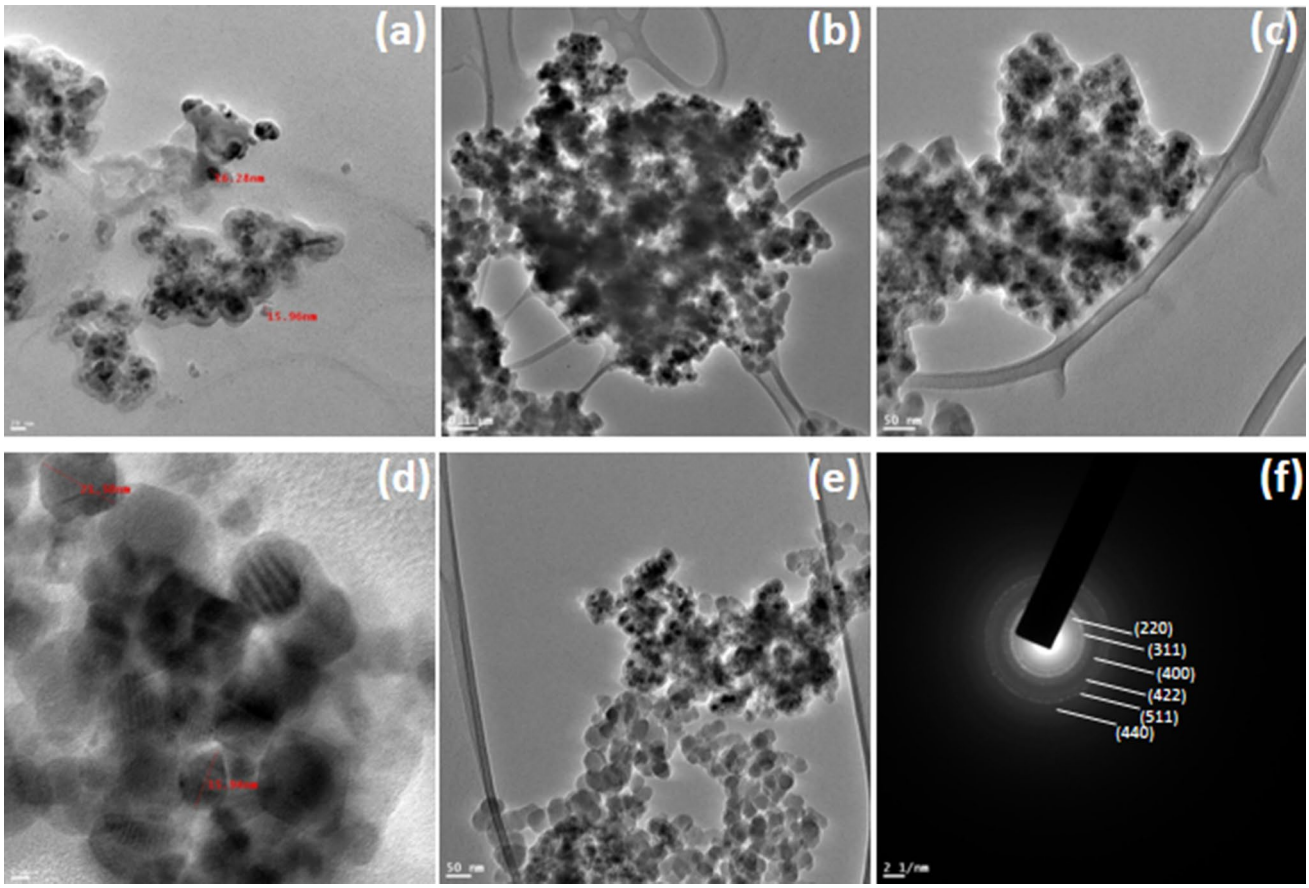

Fig. 2 **a**–**c** TEM images of as synthesized DDBSA@MNP, **d**, **e** TEM images of recycled catalyst and **f** SAED pattern of Fe_3O_4

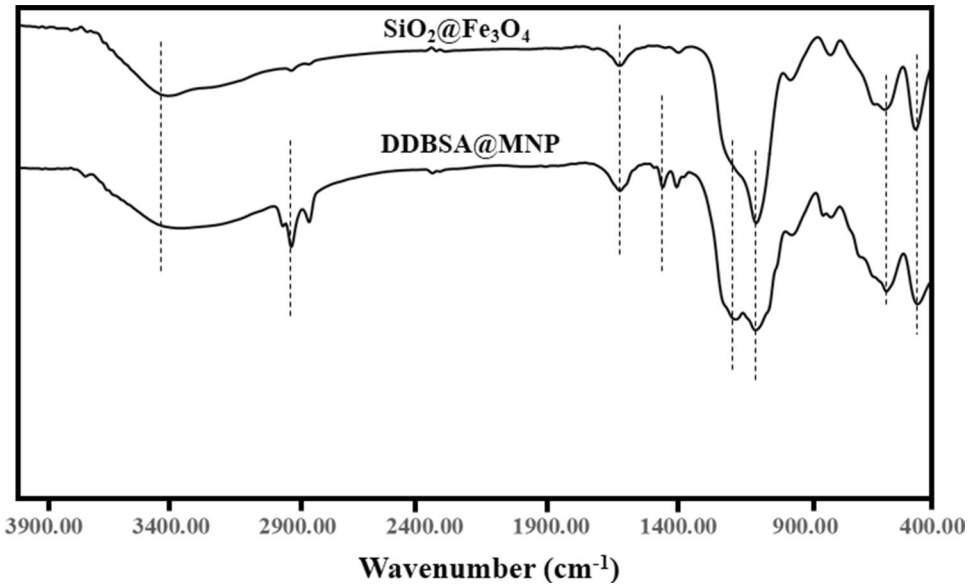

Fig. 3 FTIR spectra of SiO_2@Fe_3O_4 and DDBSA@MNP

(FESEM) technique. FESEM images of DDBSA@MNP are depicted in Fig. 4. The images show rough surface due to functionalization around core magnetite nanoparticles. Additional information regarding chemical composition of DDBSA@MNP was checked with energy-dispersive x-ray (EDX) spectroscopy. The EDX spectrum of the catalyst shows the presence of C, O, Fe, Si and S (Fig. 4), which confirms the grafting of DDBSA on SiO_2@Fe_3O_4 nanoparticles.

The thermal stability of the catalyst was investigated by thermogravimetric (TG) analysis (Fig. 5). The curve indicates an initial weight loss of 6.72% up to 100 °C, which corresponds to the silanol groups and adsorbed water on the support. Thermal degradation of the catalyst was mainly occurred between 280 and 500 °C, due to degradation of organic moiety. TG analysis revealed the excellent stability of the catalyst and also suggests the loading of 0.56 mmol g^{-1} DDBSA on SiO_2@Fe_3O_4.

The magnetic property of the catalyst was checked through vibrating sample magnetometry (VSM) analysis at room temperature (Fig. 6). The magnetization of the catalyst was found less compared to necked Fe_3O_4 nanoparticles due to silica coating and grafting of DDBSA. Nevertheless, it was sufficient for magnetic decantation of the catalyst from reaction mixture.

Catalytic efficiency of the DDBSA@MNP for the synthesis of quinolines via Friedlander reaction

The Friedlander reaction was performed to exploit the catalytic performance of DDBSA@MNP. Reaction optimization was commenced with the model reaction of 2-aminobenzophenone and ethyl acetoacetate (Table 1). Initially, the model reaction was performed in the absence of catalyst using ethanol as a solvent under reflux condition. The reaction was run for 6 h and ended with poor yield of the corresponding ethyl 2-methyl-4-phenylquinoline-3-carboxylate (Table 1, entry 1). Among the different amount of DDBSA@MNP screened, 0.15 g of catalyst shows the best results under reflux condition with ethanol (Table 1, entries 2–5). The effect of solvent on reaction was evaluated through utilizing different organic solvents and solvent-free reaction at 80 °C using optimum amount of DDBSA@MNP (Table 1, entries 6–9). The obtained results were suggested that the efficiency and the yield of reaction in ethanol were much higher than other organic solvents and solvent-free condition. The capability of DDBSA@MNP catalyst is compared with reported catalysts for the synthesis of 3a (Table 1, entries 10–14). The present catalyst is found superior than some of the reported catalysts in terms of facile catalyst recovery and reusability, easy handling, mild reaction condition and excellent isolated yields.

Generality and scope of the reaction were investigated through utilization of substituted 2-aminoaryl ketones and β-ketoester/ketone in the reaction under optimum condition, and the results are depicted in Table 2. All the reactions were monitored through TLC and yielded the corresponding products with short reaction time. Plausible mechanism of DDBSA@MNP-catalyzed Friedlander reaction is proposed (Scheme 4). It is anticipated that catalyst activates the carbonyl carbon of 2-aminoaryl ketone for the nucleophilic attack by active methylene of β-ketoester/ketone to form a product of cross-aldol reaction. The resultant β-hydroxy ketone loses water molecule to generate α,β-unsaturated ketone, which upon cyclization generates targeted quinoline derivative.

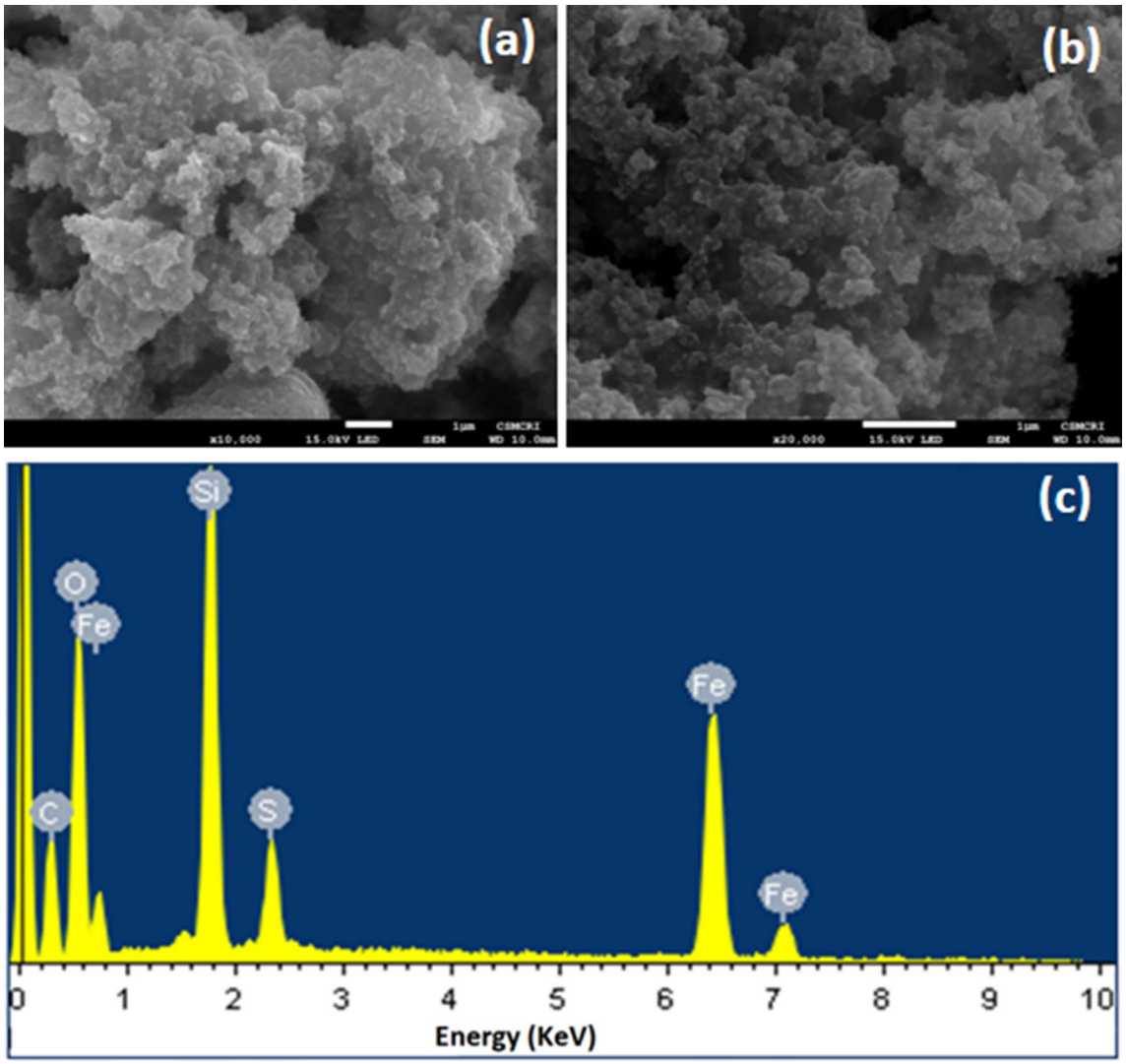

Fig. 4 **a**, **b** FESEM images of DDBSA@MNP, **c** EDX spectrum of DDBSA@MNP

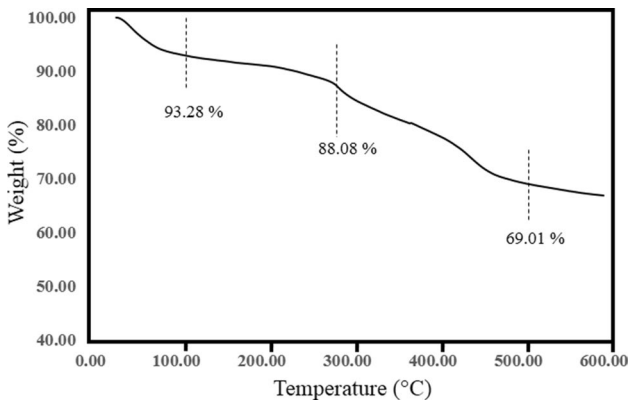

Fig. 5 TG analysis of DDBSA@MNP

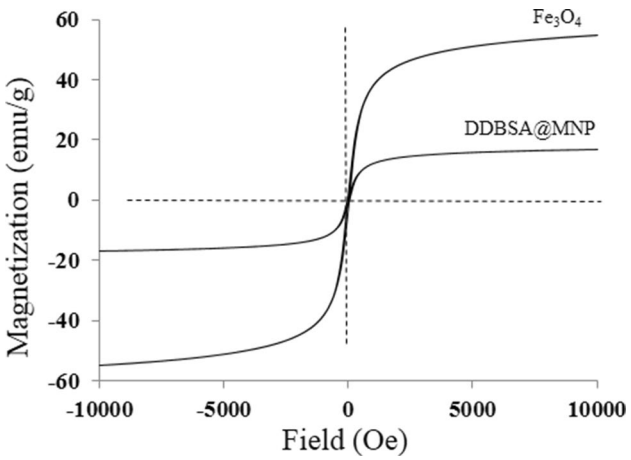

Fig. 6 Magnetization curves of Fe_3O_4 and DDBSA@MNP

Table 1 Optimization of the reaction condition for the synthesis of quinoline derivatives

Entry	Catalyst (g)	Solvent	Temperature (°C)	Time (h)	Yield (%)[a]
1	No catalyst	Ethanol	Reflux	6	–[b]
2	DDBSA@MNP (0.05)	Ethanol	Reflux	6	60
3	DDBSA@MNP (0.10)	Ethanol	Reflux	5	80
4	DDBSA@MNP (0.15)	Ethanol	Reflux	3	95
5	DDBSA@MNP (0.20)	Ethanol	Reflux	3	92
6	DDBSA@MNP (0.15)	Water	Reflux	6	74
7	DDBSA@MNP (0.15)	CH_2Cl_2	Reflux	6	68
8	DDBSA@MNP (0.15)	$CHCl_3$	Reflux	6	56
9	DDBSA@MNP (0.15)	Solvent-free	80	6	38
10	APT_{POL60}	Ethanol	Reflux	24	92 [59]
11	HCl	Water	RT	19	84 [60]
12	[Msim][$OOCCCl_3$]	No solvent	100	0.75	91 [61]
13	α-Chymotrypsin	[EMIM][BF_4]	55	24	90 [62]
14	DBSA	Water	50	2	92 [63]

Reaction condition: 2-aminobenzophenone (1 mmol) and ethyl acetoacetate (1.5 mmol)

[a]Isolated yield

[b]Poor yield

Table 2 Preparation of substituted quinoline derivatives using DDBSA@MNP as a catalyst

Product	R_1	R_2	R_3	Time (h)	Yield (%)[a]	Melting point (°C)	
						Found	Reported
3a	C_6H_5	CH_3	$CO_2C_2H_5$	3	95	100–102	99–102 [64]
3b	C_6H_5	CH_3	CO_2CH_3	4	94	98–100	99–100 [65]
3c	C_6H_5	CH_3	$COCH_3$	4	92	110–112	111–112 [64]
3d	C_6H_5	$–(CH_2)_3–$		6	90	148–150	148–149 [66]
3e	C_6H_5	$–(CH_2)_4–$		5	91	130–132	131–132 [66]
3f	C_6H_5	$–(CH_2C(CH_3)_2CH_2CO–$		4	93	190–192	189–192 [67]
3g	CH_3	CH_3	$CO_2C_2H_5$	3	90	Oil	Oil [68]
3h	CH_3	CH_3	$COCH_3$	5	86	Oil	Oil [68]
3i	CH_3	C_6H_5	H	4	90	Oil	Oil [68]
3j	CH_3	$–(CH_2)_4–$		4	90	80–82	78 [68]
3k	CH_3	$–(CH_2C(CH_3)_2CH_2CO–$		3	89	106–108	104–106 [64]

[a]Isolated yield

Catalytic efficiency of the DDBSA@MNP for the synthesis of 1-amidoalkyl-2-naphthols

The catalytic effectiveness of DDBSA@MNP was investigated for the synthesis of 1-amidoalkyl-2-naphthol derivatives. The condensation between 2-naphthol, benzaldehyde and acetamide was chosen as the model reaction under solvent-free condition (Table 3). In the beginning, the model reaction was performed without catalyst at 80 °C, and even after 60 min, no progress was observed in the reaction (Table 3, entry 1). The effect of the catalyst loading was tested through utilizing different amounts of DDBSA@MNP in the model reaction (Table 3, entries 2–5). Interestingly, it was found that the catalyst accelerates the reaction and the best result was obtained with 0.15 g catalyst (Table 3, entry 4). After that, the influence of temperature was taken into consideration for the model reaction with 0.15 g catalyst (Table 3, entries 6–7). From the optimization, it was found that the model reaction at 80 °C afforded a satisfactory yield with shorter reaction time. The catalytic efficiency of the present catalyst is compared with some recent reports for the synthesis of 7a (Table 3, entries 8–12). The DDBSA@MNP was found better as compared to some reported catalysts concerning easy recovery of catalyst through magnetic decantation, efficient reusability of the catalyst, hassle-free workup, shorter reaction time and higher yield.

With this optimum condition in hand, general adaptability of the catalyst was tested through its utilization for the synthesis of different 1-amidoalkyl-2-naphthol derivatives. As shown in Table 4, the condensation between

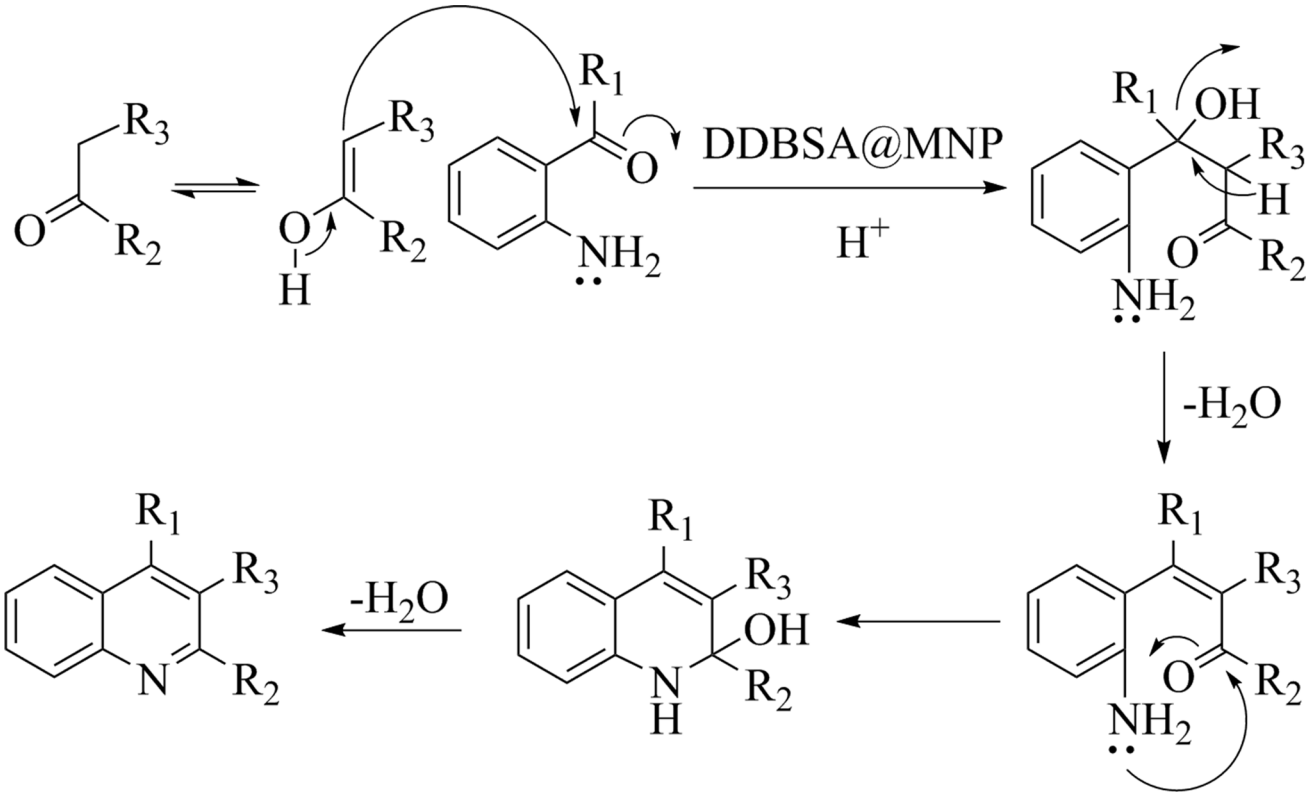

Scheme 4 Plausible mechanism for the DDBSA@MNP-catalyzed synthesis of substituted quinolines

Table 3 Optimization of the reaction condition for the synthesis of 1-amidoalkyl-2-naphthol derivatives

Entry	Catalyst (g)	Temperature (°C)	Time (min)	Yield (%)[a]
1	No catalyst	80	60	NR[b]
2	DDBSA@MNP (0.05)	80	30	64
3	DDBSA@MNP (0.10)	80	18	82
4	DDBSA@MNP (0.15)	80	12	91
5	DDBSA@MNP (0.20)	80	12	90
6	DDBSA@MNP (0.15)	60	15	86
7	DDBSA@MNP (0.15)	100	12	91
8	$[C_6(MPy)_2]$ $[CoCl_4]^{2-}$	120	25	75 [69]
9	$PhB(OH)_2$	120	180	80 [70]
10	Tetrachlorosilane	RT	15	83 [52]
11	$RGO/CoFe_2O_4$@Cu(II)	120	35	90 [71]
12	$Ba_3(PO_4)_2$	100	45	87 [72]

Reaction condition: 2-naphthol (1 mmol), benzaldehyde (1 mmol), acetamide (1.2 mmol), solvent-free

[a]Isolated yield

[b]No reaction

substituted aldehydes, amides and 2-naphthol, proceeded efficiently to achieve the corresponding products in excellent isolated yield. The proposed mechanism for DDBSA@MNP-catalyzed synthesis of 1-amidoalkyl-2-naphthol derivatives is shown in Scheme 5. Initially, the nucleophilic attack of 2-naphthol on activated aldehyde to get an intermediate, which upon removal of water molecule produce an *ortho*-quinone methide intermediate. This on reaction with amide via a Michael addition acquires the expected 1-amidoalkyl-2-naphthol derivative.

Catalyst recovery and reusability

In order to design economic and ecological favorable methodology, sustainability of the catalyst is an important factor. Therefore, the recyclability of the catalyst was investigated in both transformations through its utilization for the synthesis of ethyl 2-methyl-4-phenylquinoline-3-carboxylate and N-((2-hydroxynaphthalen-1-yl)(2-nitrophenyl)methyl) acetamide. In both reactions, the catalyst could be easily separated from the reaction mixture through external magnet after completion of reaction. The recovered catalyst was washed three times with ethanol and dried under vacuum to reuse in the subsequent reactions. As shown in Fig. 7, the catalyst was found almost equally efficient up to five reaction cycles in both tested cases. The morphology of the recovered catalyst was checked by TEM analysis (Fig. 2). TEM images of the recovered catalyst confirm that

Table 4 Preparation of 1-amidoalkyl-2-naphthol derivatives using DDBSA@MNP as a catalyst

Product	R_4	R_5	Time (min)	Yield (%)[a]	Melting point (°C)	
					Found	Reported
7a	C_6H_5–	CH_3–	12	91	241–243	239–240 [73]
7b	2-NO_2–C_6H_4–	CH_3–	10	90	237–238	218–220 [74]
7c	3-NO_2–C_6H_4–	CH_3–	10	92	256–258	256–258 [74]
7d	4-NO_2–C_6H_4–	CH_3–	10	92	237–238	248–250 [73]
7e	4-Cl–C_6H_4–	CH_3–	14	91	231–232	229–230 [75]
7f	2,4-Cl_2–C_6H_3–	CH_3–	15	89	225–228	226–228 [76]
7g	C_6H_5–	NH_2–	10	92	172–174	172–174 [50]
7h	4-Cl–C_6H_4–	NH_2–	12	88	168–169	170–172 [77]
7i	3-NO_2–C_6H_4–	NH_2–	10	91	186–188	184–186 [50]
7j	C_6H_5–	C_6H_5–	14	90	238–240	234–236 [75]
7k	4-Cl–C_6H_4–	C_6H_5–	14	89	187–188	180–182 [75]
7l	2-NO_2–C_6H_4–	C_6H_5–	12	91	266–267	266–267 [74]
7m	3-NO_2–C_6H_4–	C_6H_5–	12	90	242–243	240–242 [78]
7n	4-NO_2–C_6H_4–	C_6H_5–	10	89	228–229	228–229 [74]
7o	2,4-Cl_2–C_6H_3–	C_6H_5–	12	88	262–263	262–263 [74]

[a]Isolated yield

Scheme 5 Plausible mechanism for the DDBSA@MNP-catalyzed synthesis of 1-amidoalkyl-2-naphthols

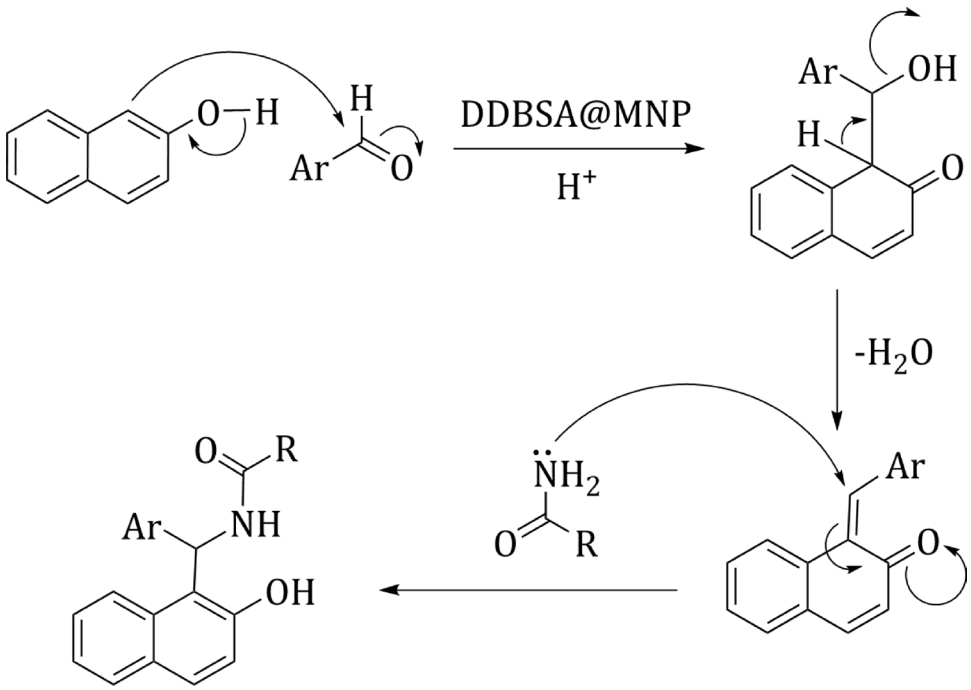

DDBSA@MNP maintained its crystallinity and size after five repeated catalytic cycles. To assess the leaching of the dodecylbenzenesulfonic acid from the DDBSA@MNP during the reaction, the solid catalyst was separated through magnetic decantation from the reaction mixture at halfway of the reaction. The reaction was continued in the absence of the catalyst for appropriate time and monitored by TLC. No further rise in the conversion was detected, which indicates the no leaching of the grafted dodecylbenzenesulfonic acid from the magnetite nanoparticles during reaction.

Conclusions

In conclusion, we have successfully synthesized dodecylbenzenesulfonic acid-grafted magnetite nanoparticles (DDBSA@MNP) and exploited its catalytic efficiency for the synthesis of substituted quinoline and 1-amidoalkyl-2-naphthol derivatives via one-pot condensation. Importantly, the catalyst could be easily separated from the reaction mixture through magnetic decantation and

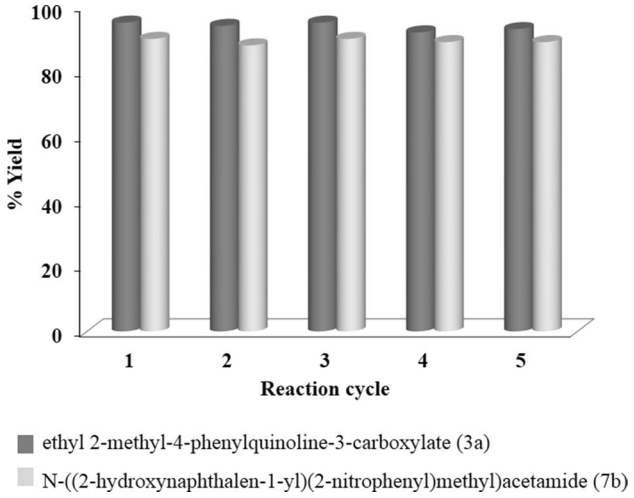

Fig. 7 Reusability of DDBSA@MNP for the synthesis of 3a and 7b

reused efficiently up to five reaction cycles in both reactions. The notable advantages such as excellent isolated yields, shorter reaction time, straightforward workup and purification make these methodologies more advantageous compared to conventional.

Acknowledgements Research facilities provided by P. D. Patel Institute of Applied Sciences, Charotar University of Science and Technology (CHARUSAT), are gratefully acknowledged. The authors are also thankful to CSMCRI, Bhavnagar, for analysis at concessional rate.

References

1. K. Sordakis, C. Tang, L.K. Vogt, H. Junge, P.J. Dyson, M. Beller, G. Laurenczy, Chem. Rev. **118**, 372 (2018)
2. P.S. Pregosin, Angew. Chem. Int. Ed. **52**, 1627 (2013)
3. P.J. Craig, Appl. Organomet. Chem. **8**, 499 (1994)
4. D.J. Cole-Hamilton, Science **299**, 1702 (2003)
5. J. Hagen, in *Industrial Catalysis: A Practical Approach*, ed. by J. Hagen (Wiley, New York, 2015), p. 47
6. M.R. Siddiqui, Z.A. AlOthman, N. Rahman, Arab. J. Chem. **10**, S1409 (2017)
7. V. Polshettiwar, R.S. Varma, Green Chem. **12**, 743 (2010)
8. F.A. Westerhaus, R.V. Jagadeesh, G. Wienhöfer, M.-M. Pohl, J. Radnik, A.-E. Surkus, J. Rabeah, K. Junge, H. Junge, M. Nielsen, A. Brückner, M. Beller, Nat. Chem. **5**, 537 (2013)
9. S.A. Dergunov, A.T. Khabiyev, S.N. Shmakov, M.D. Kim, N. Ehterami, M.C. Weiss, V.B. Birman, E. Pinkhassik, ACS Nano **10**, 11397 (2016)
10. K.A.D.F. Castro, M. Halma, G.S. Machado, G.P. Ricci, G.M. Ucoski, K.J. Ciuffi, S. Nakagaki, J. Braz, Chem. Soc. **21**, 1329 (2010)
11. A.R. Silva, M.M.A. Freitas, C. Freire, B. de Castro, J.L. Figueiredo, Langmuir **18**, 8017 (2002)
12. V.S. Shende, V.B. Saptal, B.M. Bhanage, Chem. Rec. **19**, 2022 (2019)
13. N. Kosinov, C. Liu, E.J.M. Hensen, E.A. Pidko, Chem. Mater. **30**, 3177 (2018)
14. W. Luo, W. Cao, P.C.A. Bruijnincx, L. Lin, A. Wang, T. Zhang, Green Chem. **21**, 3744 (2019)
15. D. Astruc, Chem. Rev. **120**, 461 (2020)
16. J. Govan, Y. Gun'ko, Nanomaterials **4**, 222 (2014)
17. V. Polshettiwar, R. Luque, A. Fihri, H. Zhu, M. Bouhrara, J.-M. Basset, Chem. Rev. **111**, 3036 (2011)
18. S. Shylesh, V. Schünemann, W.R. Thiel, Angew. Chem. Int. Ed. **49**, 3428 (2010)
19. M.B. Gawande, P.S. Branco, R.S. Varma, Chem. Soc. Rev. **42**, 3371 (2013)
20. P. Friedlaender, Ber. Dtsch. Chem. Ges. **15**, 2572 (1882)
21. S. Fetzner, B. Tshisuaka, F. Lingens, R. Kappl, J. Hüttermann, Angew. Chem. Int. Ed. **37**, 576 (1998)
22. O. Afzal, S. Kumar, M.R. Haider, M.R. Ali, R. Kumar, M. Jaggi, S. Bawa, Eur. J. Med. Chem. **97**, 871 (2015)
23. Y.-Q. Hu, C. Gao, S. Zhang, L. Xu, Z. Xu, L.-S. Feng, X. Wu, F. Zhao, Eur. J. Med. Chem. **139**, 22 (2017)
24. Z. Xiao, F. Lei, X. Chen, X. Wang, L. Cao, K. Ye, W. Zhu, S. Xu, Arch. Pharm. **351**, 1700407 (2018)
25. R. Abonia, D. Insuasty, J. Castillo, B. Insuasty, J. Quiroga, M. Nogueras, J. Cobo, Eur. J. Med. Chem. **57**, 29 (2012)
26. Y. Leyla, A.Ç. Gülşen, Anti-Cancer Agents Med. Chem. **18**, 1122 (2018)
27. S. Jain, V. Chandra, P. Kumar Jain, K. Pathak, D. Pathak, A. Vaidya, Arab. J. Chem. **12**, 4920 (2019)
28. M. Kidwai, N. Negi, Monatshefte Chem. Chem. Mon. **128**, 85 (1997)
29. N. von Rosenstiel, D. Adam, Drugs **47**, 872 (1994)
30. D. Bouzard, P. Di Cesare, M. Essiz, J.P. Jacquet, J.R. Kiechel, P. Remuzon, A. Weber, T. Oki, M. Masuyoshi, J. Med. Chem. **33**, 1344 (1990)
31. R. Musiol, M. Serda, S. Hensel-Bielowka, J. Polanski, Curr. Med. Chem. **17**, 1960 (2010)
32. H. Cairns, D. Cox, K.J. Gould, A.H. Ingall, J.L. Suschitzky, J. Med. Chem. **28**, 1832 (1985)
33. A. Kumar, K. Srivastava, S. Raja Kumar, S.K. Puri, P.M.S. Chauhan, Bioorgan. Med. Chem. Lett. **20**, 7059 (2010)
34. J.S. Wolfson, D.C. Hooper, Clin. Microbiol. Rev. **2**, 378 (1989)
35. S.K. Suthar, V. Jaiswal, S. Lohan, S. Bansal, A. Chaudhary, A. Tiwari, A.T. Alex, A. Joesph, Eur. J. Med. Chem. **63**, 589 (2013)
36. Y.-L. Fan, J.-B. Wu, X.-W. Cheng, F.-Z. Zhang, L.-S. Feng, Eur. J. Med. Chem. **146**, 554 (2018)
37. E.A. Fehnel, J. Org. Chem. **31**, 2899 (1966)
38. C.-S. Jia, Z. Zhang, S.-J. Tu, G.-W. Wang, Org. Biomol. Chem. **4**, 104 (2006)
39. J.S. Yadav, B.V.S. Reddy, K. Premalatha, Synlett **2004**, 963 (2004)
40. D.S. Bose, R.K. Kumar, Tetrahedron Lett. **47**, 813 (2006)
41. S.K. De, R.A. Gibbs, Tetrahedron Lett. **46**, 1647 (2005)
42. K. Mogilaiah, C.S. Reddy, Synth. Commun. **33**, 3131 (2003)
43. A.Y. Shen, C.T. Tsai, C.L. Chen, Eur. J. Med. Chem. **34**, 877 (1999)
44. S. Knapp, Chem. Rev. **95**, 1859 (1995)
45. Y.F. Wang, T. Izawa, S. Kobayashi, M. Ohno, J. Am. Chem. Soc. **104**, 6465 (1982)
46. D. Seebach, J.L. Matthews, Chem. Commun. **21**, 2015–2022 (1997)
47. M.M. Khodaei, A.R. Khosropour, H. Moghanian, Synlett **2006**, 916 (2006)
48. Z. Karimi-Jaberi, M. Jokar, S. Abbasi, J. Chem. **2013**, 1 (2012)
49. H.R. Shaterian, H. Yarahmadi, M. Ghashang, Bioorg. Med. Chem. Lett. **18**, 788 (2008)
50. S.B. Patil, P.R. Singh, M.P. Surpur, S.D. Samant, Ultrason. Sonochem. **14**, 515 (2007)
51. H.R. Shaterian, A. Amirzadeh, F. Khorami, M. Ghashang, Synth. Commun. **38**, 2983 (2008)

52. S.B. Said, M.M. Mashaly, A.M. Sheta, S.S. Elmorsy, Int. J. Org. Chem. **5**, 191 (2015)
53. M.B. Gawande, A. Rathi, I.D. Nogueira, C.A.A. Ghumman, N. Bundaleski, O.M.N.D. Teodoro, P.S. Branco, ChemPlusChem **77**, 865 (2012)
54. A. Tiwari, A. Singh, A. Debnath, A. Kaul, N. Garg, R. Mathur, A. Singh, J.K. Randhawa, ACS Appl. Nano Mater. **2**, 3060 (2019)
55. R.L. Frost, O.B. Locos, H. Ruan, J.T. Kloprogge, Vib. Spectrosc. **27**, 1 (2001)
56. Y. Liu, P. Liu, Z. Su, F. Li, F. Wen, Appl. Surf. Sci. **255**, 2020 (2008)
57. J. Wang, S. Zheng, Y. Shao, J. Liu, Z. Xu, D. Zhu, J. Colloid Interface Sci. **349**, 293 (2010)
58. P. Larkin, in *Infrared and Raman Spectroscopy*, ed. by P. Larkin (Elsevier, Oxford, 2011), p. 73
59. D.O. Bennardi, M.N. Blanco, L.R. Pizzio, J.C. Autino, G.P. Romanelli, Curr. Catal. **4**, 65 (2015)
60. P. Gopi, S. Sarveswari, Monatshefte Chem. **148**, 1043 (2017)
61. P. Sarma, A.K. Dutta, P. Gogoi, B. Sarma, R. Borah, Monatshefte Chem. **146**, 173 (2015)
62. Z.-G. Le, M. Liang, Z.-S. Chen, S.-H. Zhang, Z.-B. Xie, Molecules **22**, 762 (2017)
63. B. Tanwar, A. Kumar, P. Yogeeswari, D. Sriram, A.K. Chakraborti, Bioorg. Med. Chem. Lett. **26**, 5960 (2016)
64. D.S. Bose, M. Idrees, N.M. Jakka, J.V. Rao, J. Comb. Chem. **12**, 100 (2010)
65. M. Dabiri, S. Bashiribod, Molecules **14**, 1126 (2009)
66. J. Akbari, A. Heydari, H. Reza Kalhor, S.A. Kohan, J. Comb. Chem. **12**, 137 (2010)
67. M. Narasimhulu, T.S. Reddy, K.C. Mahesh, P. Prabhakar, C.B. Rao, Y. Venkateswarlu, J. Mol. Catal. A: Chem. **266**, 114 (2007)
68. S.S. Palimkar, S.A. Siddiqui, T. Daniel, R.J. Lahoti, K.V. Srinivasan, J. Org. Chem. **68**, 9371 (2003)
69. A. Chinnappan, A.H. Jadhav, W.-J. Chung, H. Kim, J. Mol. Liq. **212**, 413 (2015)
70. K. Boudebbous, H. Boulebd, C. Bensouici, D. Harakat, R. Boulcina, A. Debache, ChemistrySelect **5**, 5515 (2020)
71. M. Kooti, M. Karimi, E. Nasiri, J. Nanopart. Res. **20**, 16 (2018)
72. H. Taghrir, M. Ghashang, M.N. Biregan, Chin. Chem. Lett. **27**, 119 (2016)
73. A. Zare, T. Yousofi, A.R. Moosavi-Zare, RSC Adv. **2**, 7988 (2012)
74. G.C. Nandi, S. Samai, R. Kumar, M.S. Singh, Tetrahedron Lett. **50**, 7220 (2009)
75. A.R. Hajipour, Y. Ghayeb, N. Sheikhan, A.E. Ruoho, Tetrahedron Lett. **50**, 5649 (2009)
76. H. Khabazzadeh, K. Saidi, N. Seyedi, J. Chem. Sci. **121**, 429 (2009)
77. Z. Nasresfahani, M.Z. Kassaee, E. Eidi, New J. Chem. **40**, 4720 (2016)
78. M. Zandi, A.R. Sardarian, C. R. Chim. **15**, 365 (2012)